

FREQUENCY BEHAVIOR OF A SHIELDED LOOP ANTENNA WITH A VARIABLE GAP POSITION

K. Maurer ⁽¹⁾, C. D. Nordquist ⁽²⁾, and J.T. Bernhard ⁽¹⁾

(1) Electromagnetics Laboratory, University of Illinois at Urbana-Champaign

(2) Sandia National Laboratories

ABSTRACT: When taking near field measurements for electromagnetic interference detection, the shielded loop is often employed due to its ability to suppress common mode currents, which aids in the measurements taken of the magnetic field. This work investigates the frequency behavior of a shielded loop antenna when the gap position is changed, focusing on the electrical length from the gap to the shorted end of the loop. This length corresponds to the resonance of the loop, first at approximately two fifths wavelength followed by each additional half wavelength.

1. Introduction

Electromagnetic interference (EMI) testing is often done in order for components to pass regulatory standards for emission. Given the rapidly increasing density of electronic modules, it is advantageous to analyze this EMI during the design and prototyping stage as it can allow for early identification of potential faults in the system. Far field measurements prove inefficient at characterizing and predicting the performance of high-density microsystems at a chip and module level as the localization of emissions sources cannot be as specific when measured from the far field. By instead measuring in the near field, the proximity to the device under test lends itself to much higher resolution and can pinpoint these emissions sources to debug. A common structure used in this near field scanning is the shielded loop, which measures the magnetic field. This is useful as the shielded magnetic probe can more easily suppress common mode currents due to the electric field and reduce noise which can aid the sensitivity of the probe [1]. An example of this is the work done by Tohoku University in miniaturized thin film magnetic probes which employ micrometer geometry and achieve high spatial resolution using the shielded loop [2]. Figure 1 shows an iteration of the design from [2] which can achieve up to 10 μm spatial resolution, and a bandwidth of approximately 100 MHz to 3 GHz, where the upper limit of this bandwidth is inhibited by the need for a low noise amplifier that is cut off above 3 GHz. Based on this and other shielded loops, this is the best starting point for the design of our own near field probe, with the intention of gaining a better understanding of the

structure and the degrees of freedom that it may allow. In the first available model of the shielded loop, the loop is treated as a coaxial transmission line with the perimeter of a quarter wavelength [3]. However, rather than adhering to the original design, we investigate the frequency response of the structure while varying the position of the shield gap.

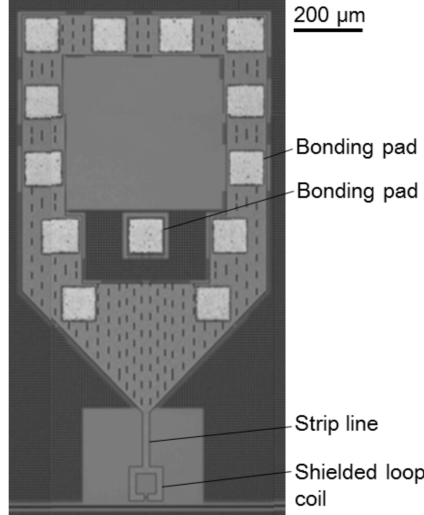


Figure 1. Tohoku 60 μm x 60 μm shielded loop [2]

2. Shielded Loop Geometry

The shielded loop is constructed using a coaxial cable model. The outer conductor is grounded, while the inner conductor is shorted to the outer conductor at the end of the loop. The outer conductor of a shielded loop has a gap typically located opposite the feed input where the signal is received and so that the entire loop is not shorted to ground.

The gap position is defined by its angular location on the loop, where the farthest end from the feed line is designated as 180° , and the position directly opposite is defined as 0° . Figure 2 shows the gap in the position designated as 180° , where most shielded loops locate the gap in the outer conductor and rely on the total loop circumference rather than adjusting the location of this gap.

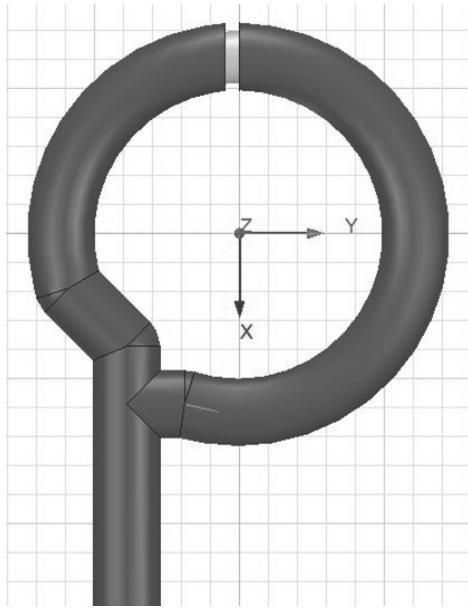


Figure 2. Base HFSS model of simulated shielded loop with gap at 180°

What we are specifically interested in is how changing this gap location effects the behavior of the loop without changing the loop radius, and how this relates to the electrical length between the shorted end of the loop and the gap. The coaxial cable has an inner conductor diameter of 0.28 mm, a dielectric diameter of 0.91 mm, and an outer diameter of 1.17 mm. The dielectric is fluorinated ethylene propylene (FEP) with a relative permittivity of 2.1. The loop radius is 3.05 mm, and the width of the shield gap is 0.25 mm. The length between the short and the gap is measured along the center of the inner conductor, beginning directly at the short to the edge of the gap closest to the short. The radius of 3.05 mm is measured from the center of the loop to the center of the inner conductor and is used to calculate this length of interest.

This base model is similar to the vast majority of shielded loops in use, given the gap location. Using this as the base, we can now move the gap to various angle positions to examine the frequency behavior of this loop and its correlation to the length between the gap and the short.

3. Frequency Behavior Investigation

In this simulation study, the gap is repositioned to three different angles, 90°, 130°, and 150°, as shown in Figures 3 – 5. When examining the S_{11} plot in Figure 6, the pattern becomes clear when examining the length of interest. The farther from the short the gap is located, the lower the initial resonant frequency is. Table 1 maps the initial frequency response of the shielded loop at each gap position, each with the same gap width. The electrical length is designated by the length between the shorted end of the inner conductor

to the beginning edge of the gap divided by the wavelength of the first resonant frequency according to the S_{11} plot. This wavelength is calculated using equation 1.

$$\lambda_f = \frac{c}{f\sqrt{\epsilon_r}} \quad (1)$$

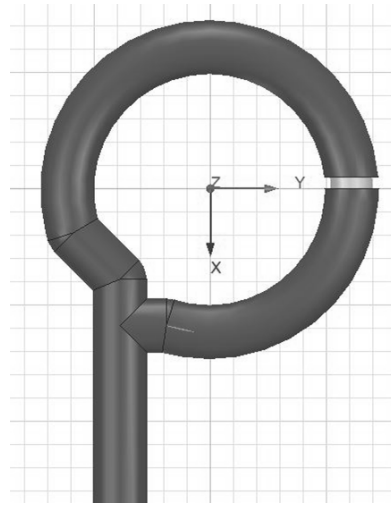


Figure 3. HFSS model of simulated shielded loop with gap at 90°

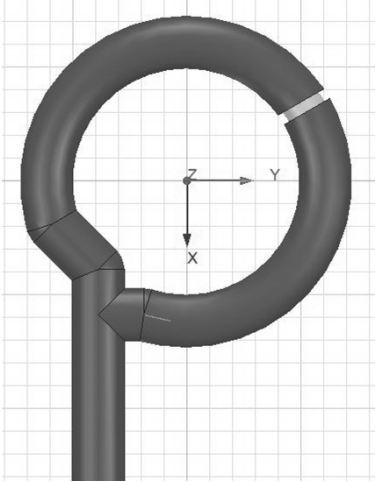


Figure 4. HFSS model of simulated shielded loop with gap at 120°

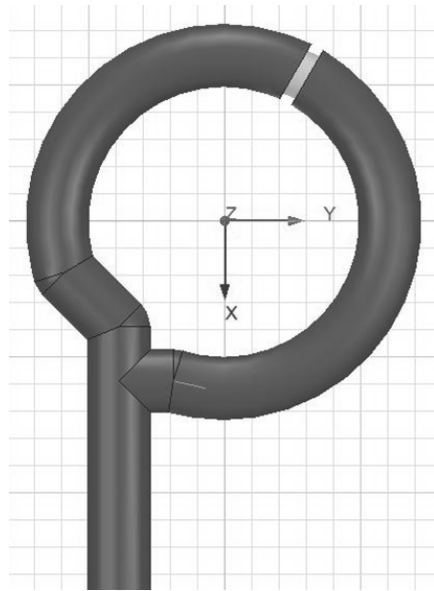


Figure 5. HFSS model of simulated shielded loop with gap at 150°

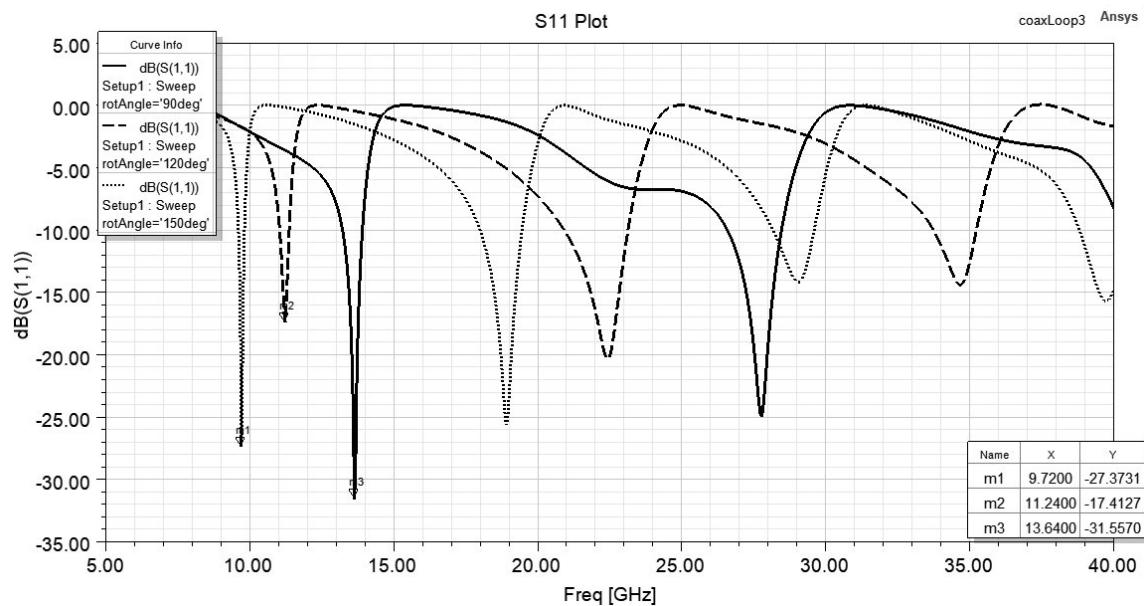


Figure 6. S₁₁ plot for varying gap positions

Table 1. Electrical length from gap to short

Gap Position	Resonance [GHz]	Length from Short [λ]
90°	13.64	0.404
120°	11.24	0.419
150°	9.72	0.436

4. Scaling to Different Coaxial Dimensions

To examine this pattern further, we can change the geometry of the coaxial cable being used and attempt to achieve the same frequency behavior as the original model tested. In this case, changing the cable to a $50\ \Omega$ air line rather than the FEP dielectric but keeping the same loop radius and inner conductor diameter. After changing this, because the electrical length should remain the same rather than the physical length, we can obtain the physical distance from the short required on the air line using the electrical length from Table 1 to get the same resonant frequencies as the 90° base model loop.

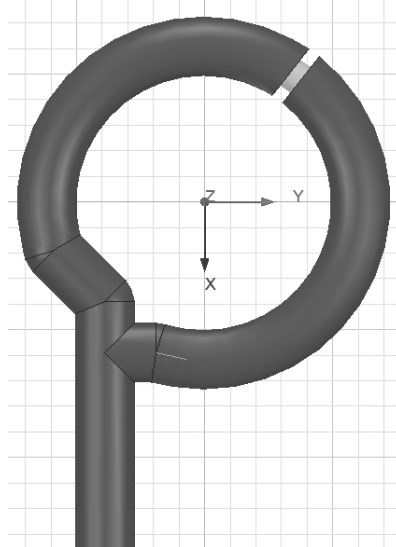


Figure 7. Adjusted air coaxial cable for 13.64 GHz initial resonance

Using the values from table 1 in the 90° position, we can aim for the same initial resonant frequency of 13.64 GHz by recalculating the distance required between the gap and the short using the new cable dielectric constant and the electrical length in Table 1. The results are displayed by comparing Figures 8 and 9, where the initial resonant frequency is within 40 MHz of each other despite the gap location variance, simply because the electrical length is the same on both structures. This further supports the observation that the distance between the shorted end of the loop and the gap location is the dimension that dictates the frequency behavior of a shielded loop.

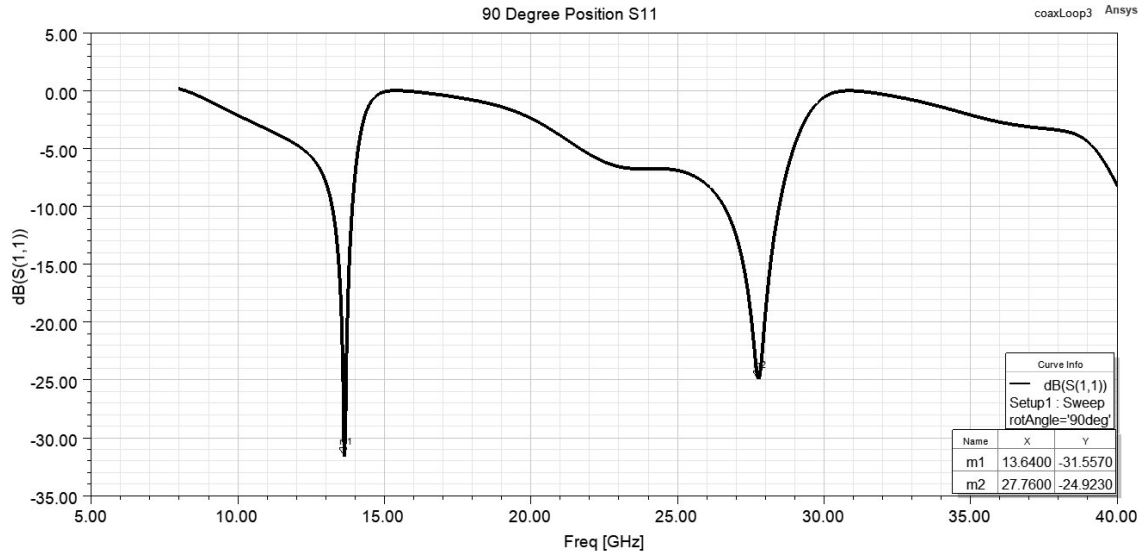


Figure 8. Original coax 90° position S_{11}

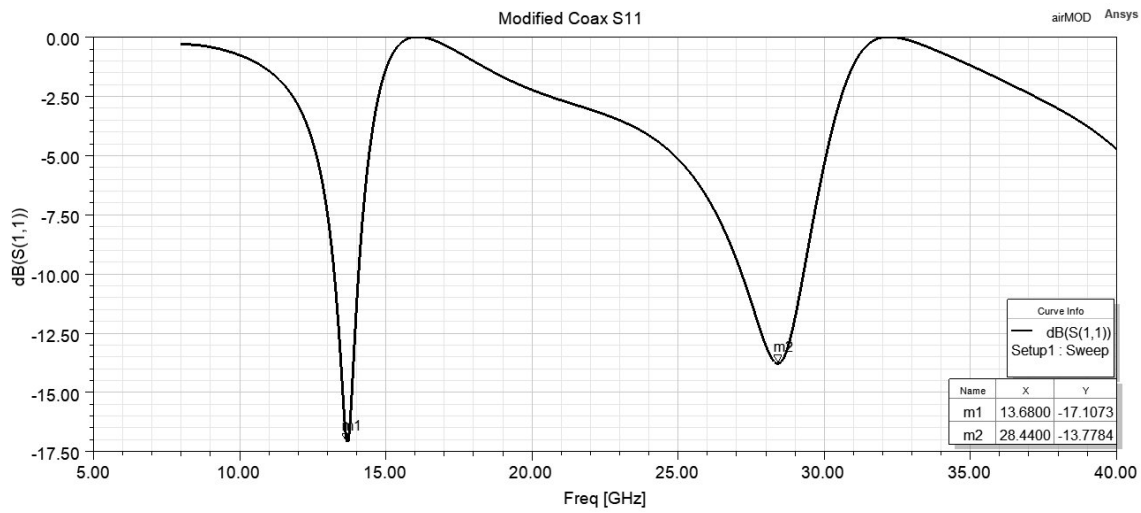


Figure 9. Air coax adjusted for 13.64 GHz initial resonance

5. Conclusion and Future Work

The frequency behavior of the shielded loop does not depend on the perimeter of the entire loop, but rather on the electrical length between the gap and the short to ground. There are many possible applications of this structure, with potential to array these loops in order to achieve increased localization of circuit board emissions.

This work was supported by the Laboratory Directed Research and Development program at Sandia National Laboratories, a multimission laboratory managed and operated by National Technology and Engineering Solutions of Sandia LLC, a wholly owned

subsidiary of Honeywell International Inc. for the U.S. Department of Energy's National Nuclear Security Administration under contract DE-NA0003525

6. References

- [1] Sivaraman, Nimisha. (2017). Design of magnetic probes for near field measurements and the development of algorithms for the prediction of EMC. *Compatibility*, 2013, pp. 977-980
- [2] M. Yamaguchi, S. Muroga, S. Nanba, K. Arai, K. Yanagi and Y. Endo, "A $60 \times 60 \mu\text{m}^2$ size planar shielded loop probe for low lift-off on-chip magnetic near field measurements," 2013 *International Symposium on Electromagnetic Compatibility*, 2013, pp. 977-980
- [3] L. L. Libby, "Special Aspects of Balanced Shielded Loops," in *Proceedings of the IRE*, vol. 34, no. 9, pp. 641-646, Sept. 1946, doi: 10.1109/JRPROC.1946.230887.